Postnatal development of synaptic transmission in local networks of L5A pyramidal neurons in rat somatosensory cortex

Andreas Frick[1], Dirk Feldmeyer[1,2] and Bert Sakmann[1]

[1]*Abteilung Zellphysiologie, Max-Planck-Institut für Medizinische Forschung, D-69120 Heidelberg, Germany*
[2]*Research Centre Juelich, Institute of Neuroscience and Biophysics INB-3, Department of Medicine, D-52425 Juelich, Germany*

The probability of synaptic transmitter release determines the spread of excitation and the possible range of computations at unitary connections. To investigate whether synaptic properties between neocortical pyramidal neurons change during the assembly period of cortical circuits, whole-cell voltage recordings were made simultaneously from two layer 5A (L5A) pyramidal neurons within the cortical columns of rat barrel cortex. We found that synaptic transmission between L5A pyramidal neurons is very reliable between 2 and 3 weeks of postnatal development with a mean unitary EPSP amplitude of ∼1.2 mV, but becomes less efficient and fails more frequently in the more mature cortex of ∼4 weeks of age with a mean unitary EPSP amplitude of 0.65 mV. Coefficient of variation and failure rate increase as the unitary EPSP amplitude decreases during development. The paired-pulse ratio (PPR) of synaptic efficacy at 10 Hz changes from 0.7 to 1.04. Despite the overall increase in PPR, short-term plasticity displays a large variability at 4 weeks, ranging from strong depression to strong facilitation (PPR, range 0.6–2.1), suggesting the potential for use-dependent modifications at this intracortical synapse. In conclusion, the transmitter release probability at the L5A–L5A connection is developmentally regulated in such a way that in juvenile animals excitation by single action potentials is efficiently transmitted, whereas in the more mature cortex synapses might be endowed with a diversity of filtering characteristics.

(Received 29 July 2007; accepted after revision 27 September 2007; first published online 4 October 2007)
Corresponding author A. Frick: Max-Planck-Institut für Medizinische Forschung, Abteilung Zellphysiologie, Jahnstrasse 29, 69120 Heidelberg, Germany. Email: andreas.frick@mpimf-heidelberg.mpg.de

Sensory cortical circuits are shaped during development in an experience-dependent and -independent manner to give rise to highly organized maps that represent the external world (Goodman & Shatz, 1993; Katz & Shatz, 1996). A useful model system for studying synaptic mechanisms underlying such a developmental formation and refinement of cortical maps is the rodent somatosensory barrel cortex because the arrangement of the whiskers on the snout is preserved in the topographical organization of neurons into barrel columns (Woolsey & van der Loos, 1970). Cortical columns are the fundamental units of organization of mammalian sensory cortices (Mountcastle, 1997; Nelson, 2002; Douglas & Martin, 2004), and barrel columns are particularly suited to examine specific columnar connections between well-defined cell types. Knowledge of the anatomical and physiological properties of several cortical connections has been recently gained using simultaneous intracellular recordings of synaptically connected cells (for reviews see: Silberberg *et al.* 2005; Watts & Thomson, 2005; Lübke & Feldmeyer, 2007). The majority of these studies were done at early developmental stages between 2 and 3 weeks of age, primarily due to experimental advantages and for comparison of diverse connections at a particular developmental stage. This period is, however, characterized by strong cortical synaptogenesis (Micheva & Beaulieu, 1996; DeFelipe *et al.* 1997), and the formation and refinement of cortical circuitry ensues to a considerable degree after this early postnatal stage (for reviews see: Cohen-Cory, 2002; Garner *et al.* 2006). In order to understand the spread of activity in columnar circuits in young and more mature cortex, it is therefore essential to study the properties of specific connections during ongoing refinement of cortical circuitry (Angulo *et al.* 1999; Reyes & Sakmann, 1999).

Layer 5 (L5) constitutes a major output layer to other cortical areas as well as subcortical regions. However, the principal neurons within this layer are not a homogenous population but can be distinguished based on their position, morphology, afferent connections and axonal

 DOI: 10.1113/jphysiol.2007.141788

projections (Wise & Jones, 1977; Zilles & Wree, 1995; Ahissar *et al.* 2001; Manns *et al.* 2004; Feldmeyer *et al.* 2005; Bureau *et al.* 2006; Larsen & Callaway, 2006; Schubert *et al.* 2006; de Kock *et al.* 2007; Frick *et al.* 2007), justifying a division of layer 5 into the sublayers L5A and L5B. Within the networks of the rat barrel cortex, L5A pyramidal neurons may act as a 'node' because they summate sensory signals arriving via the parallel lemniscal and paralemniscal thalamic pathways at early stages of cortical signal processing (Feldmeyer *et al.* 2005; Schubert *et al.* 2006). In turn, they provide intracortical (Donoghue & Parham, 1983; Koralek *et al.* 1990; Alloway *et al.* 2004; Hoffer *et al.* 2005) as well as cortical output projections to subcortical areas (Chmielowska *et al.* 1989; Mercier *et al.* 1990; Alloway *et al.* 1999; Hoffer *et al.* 2005).

We examined the synaptic properties of unitary connections at different developmental stages because of their important implications for understanding the spread of activity in the neuronal circuits of a cortical column and the mechanisms underlying the assembly of cortical circuits. Specifically, we investigated the physiology of L5A pyramidal neuron connections during postnatal development using simultaneous intracellular recordings from synaptically coupled pairs. We found that unitary EPSPs become weaker, more variable, and less reliable between the second and fourth week of postnatal development, and that the short-term plasticity changes from depression to overall slight facilitation. The most prominent functional change at this unitary connection occurred after the third week of age. Our results support the idea that the probability of release from presynaptic terminals is altered during maturation, supporting a larger range of filtering characteristics at unitary L5A–L5A connections. The consequences of these changes are discussed in the context of functional connectivity in the local networks of L5A pyramidal neurons.

Methods

Brain slices and extracellular solutions

All experimental procedures were approved by the Animal Research Committee of the Max Planck Society and complied with the guidelines laid out in the EU directive regarding the protection of animals used for experimental and scientific purposes. Wistar rats (14–29 days old) were anaesthetized with isofluorane, decapitated and neocortical slices (350 μm thick) from the barrel field of the somatosensory cortex were prepared in ice-cold extracellular solution. Brain slices were incubated at 36°C for 10–30 min in a solution containing (mM): 125 NaCl, 25 $NaHCO_3$, 2.5 KCl, 1.25 NaH_2PO_4, 6 $MgCl_2$, 1 $CaCl_2$, 3 myo-inositol, 2 sodium pyruvate, 0.4 ascorbic acid and 25 glucose. The extracellular recording solution contained 125 mM NaCl, 25 mM $NaHCO_3$, 2.5 mM KCl, 1.25 mM NaH_2PO_4, 1 mM $MgCl_2$, 2 mM $CaCl_2$ and 25 mM glucose, and was saturated with 95% O_2–5% CO_2 (pH 7.4).

Cell identification and electrophysiology

The whisker-related barrel field in layer 4 of the primary somatosensory cortex was identified at low magnification (2.5×) under bright-field illumination. Neurons were visualized with differential interference contrast (DIC) microscopy using a Zeiss Axioskop FS I microscope fitted with a 60 × 0.90 numerical aperture water-immersion objective (Olympus). Recordings were made at 33–36°C. Pipettes (4–6 MΩ) were pulled from borosilicate glass and filled with a recording solution containing (mM): 135 potassium gluconate, 10 Hepes, 10 phosphocreatine-Na, 4 KCl, 4 ATP-Mg and 0.3 guanosine triphosphate, pH 7.2 (adjusted with KOH). Biocytin (1.5–2.5 mg ml^{-1}, Sigma, Munich, Germany) was included in the recording solution for later morphological analysis. Voltage–current (*V–I*) relationships were constructed from a series of 600 ms hyperpolarizing and depolarizing current injections within the linear range of the membrane potential ($\leq \pm 5$ mV of resting potential). Linear regression analysis of *V–I* relationships was used to determine the input resistance (R_N) of each cell. The membrane time constant (τ_m) was determined by fitting the change in membrane potential (< 2 mV) induced by small hyperpolarizing and depolarizing current steps to a single exponential function. Monosynaptic connections were established by recording from the postsynaptic neuron in the whole-cell patch-clamp configuration while searching for a presynaptic partner using the 'loose-seal' technique (Feldmeyer *et al.* 1999). Once a projecting neuron was found, it was then re-patched using the whole-cell configuration. To quantify short-term changes in synaptic efficacy, we triggered bursts of three presynaptic action potentials at 10 Hz and measured changes in unitary EPSP amplitude within the train by calculating the paired-pulse ratio (PPR) of the EPSP amplitudes ($EPSP_X/EPSP_1$, with *X* denoting the position of the EPSP during a burst). Signals were recorded using Axoclamp-2B and Axopatch 200B amplifiers (Axon Instruments), low-pass filtered at 3 kHz and sampled at 10–50 kHz. Traces were acquired and analysed using commercial software (Igor Pro; WaveMetrics, Lake Oswego, OR, USA) with custom-written algorithms. Group data are expressed as mean ± S.D. unless otherwise stated, and statistical significance was calculated using non-parametric statistical tests (Mann–Whitney test).

Histological procedures

After recording, biocytin-filled neurons were processed using standard procedures previously described

(Feldmeyer *et al.* 2005). Slices were fixed at 4°C for at least 24 h in PBS containing 4% paraformaldehyde, then incubated in 0.1% Triton X-100 solution containing avidin-biotinylated horseradish peroxidase (ABC-Elite; Camon, Wiesbaden, Germany). Subsequently, 3,3-diaminobenzidine was used as reactive chromogen until axons and dendrites were clearly visible (after 2–4 min). To enhance staining contrast, slices were occasionally postfixed in 0.5% OsO_4 for up to 30–40 min before mounting on slides and embedding using Moviol (Clariant, Sulzbach, Germany). Neurons were reconstructed using Neurolucida software (MicroBrightField, Colchester, VT, USA) using an Olympus Optical (Hamburg, Germany) BX51 microscope equipped with a 100 × 1.25 numerical aperture oil-immersion objective (Lübke *et al.* 2003). No corrections for shrinkage were made. To determine the position of the labelled neurons with respect to the barrels in layer 4, barrels were visualized during the experiment (see above) and *post hoc* using the cytochrome oxidase staining according to Wong-Riley, 1979).

Results

The general protocol for these experiments was as follows. L5A pyramidal neurons in neocortical slices from 2- to 4-week-old rats (P14–P29) were identified under infrared differential interference contrast imaging (IR-DIC) video microscopy based on their position within the barrel column and on morphological criteria (Fig. 1*A*). Selected neurons fell into the 'slender-tufted' (Manns *et al.* 2004; Frick *et al.* 2007; de Kock *et al.* 2007) category that is equivalent to the 'tall-simple' category of the Larsen and Callaway classification scheme (Larsen & Callaway, 2006). Dual whole-cell voltage recordings were made from the somata of synaptically connected neurons with biocytin-filled pipettes. The majority of the presynaptic neuron somata were closer to the L4–L5A border (distance $38 \pm 27\ \mu$m, range 0–102 μm) and separated from the postsynaptic ones by $36 \pm 30\ \mu$m (range 0–135 μm, $n = 28$). Since the likelihood of finding L5A–L5A connections strongly decreased with age, we did not investigate connections in animals older than 4 weeks. The L5A–L5A connections were divided into three groups on the basis of age: postnatal day (P) 14–16, P17–20 and P24–29 (illustrated in Fig. 1*C*). Action potentials (APs) were evoked in the presynaptic neuron to elicit unitary EPSPs in the postsynaptic neuron. The majority (∼90%) of synaptically coupled pairs were uni-directionally connected, and only a small fraction (∼10%) bi-directionally. For each connection, the analysis of the synaptic properties was based on 40–200 consecutive sweeps of unitary EPSPs evoked at a repetition rate of 0.05–0.1 Hz, at which there was no obvious rundown (e.g. Figure 2*Ab*). The efficacy of a connection was determined by calculating the mean EPSP amplitude including failures of transmission, and the reliability was determined as the percentage of failures occurring and as the coefficient of variation (CV) of the EPSP amplitude. Brain slices with biocytin-filled neurons were subsequently processed histochemically to obtain more detailed information on the identity, morphology and location within the barrel column of the neurons (Fig. 1*A*, see Methods). The data were obtained from the recordings of 80 synaptically coupled pairs. Some of the data for the P17–20 age group were published in a previous study (Frick *et al.* 2007) and are used to complete the development of unitary EPSP properties between 2 and 4 weeks of age.

Decrease in input resistance during early postnatal development

First, we characterized the development of AP firing properties (Fig. 1*B*) and input resistance (R_N, Fig. 1*C*). Figure 1*B* shows an overlay of membrane voltage responses evoked by injecting a series of 600-ms-long hyper- and depolarizing current pulses through the whole-cell pipette for a connection at P15 (left panel) and another one at P28 (right panel). Typically, the membrane potential displayed a hyperpolarizing sag in response to negative current injection, and the neurons responded with a regular AP firing pattern to supra-threshold depolarizations at all ages tested. Only few neurons (∼5%, no obvious age bias) showed an intrinsically bursting pattern, responding to suprathreshold current injection with a doublet of APs at high inter-AP frequencies of 60–260 Hz. Between the second and fourth postnatal week a decline in R_N by more than 40% was observed. At P14–P16, R_N ranged from 65 to 303 MΩ with a mean of 144 ± 57 MΩ ($n = 37$, Fig. 1*C*). It decreased and became more homogenous during maturation (P17–20, 90 ± 30 MΩ, $n = 33$, $P < 0.0001$; P24–29, 83 ± 28 MΩ, $n = 28$, $P < 0.0001$) (Fig. 1*C* and Table 1). The membrane time constant (τ_m) followed a similar developmental time course as R_N. τ_m dropped from 20.6 ± 4.0 ms at P14–16 ($n = 15$) to 13.8 ± 2.6 ms at P17–20 ($n = 8$) to 12.1 ± 2.7 ms at P24–29 ($n = 14$). Thus, the major change in R_N (and τ_m) occurred during the first 3 weeks of postnatal development, and there was only a small decrease (not significant, $P = 0.36$) between 3 and 4 weeks of age. These findings are consistent with a recent study on the maturation of L5 pyramidal neurons in the rat prefrontal cortex (Zhang, 2004).

Decreased unitary EPSP amplitude in more mature cortex

To investigate whether the synaptic properties between neocortical pyramidal neurons change during the assembly period of cortical circuits, unitary EPSPs were

analysed in synaptically coupled pairs of L5A pyramidal neurons as a function of age. The results from two experiments are illustrated in Fig. 2*A*. Seven consecutive unitary EPSPs and the average response for one connection each at P15 (left panel) and P28 (right panel) are shown in Fig. 2*Aa*. A typical finding from most of our experiments and represented in this example was that, at P15, unitary EPSPs were reliably evoked with fairly high efficacy and displayed a small coefficient of variation (CV) in the EPSP amplitude. In contrast, unitary EPSPs evoked at P28 were small, characterized by large amplitude fluctuations, and occasionally failed to respond to a presynaptic AP (see

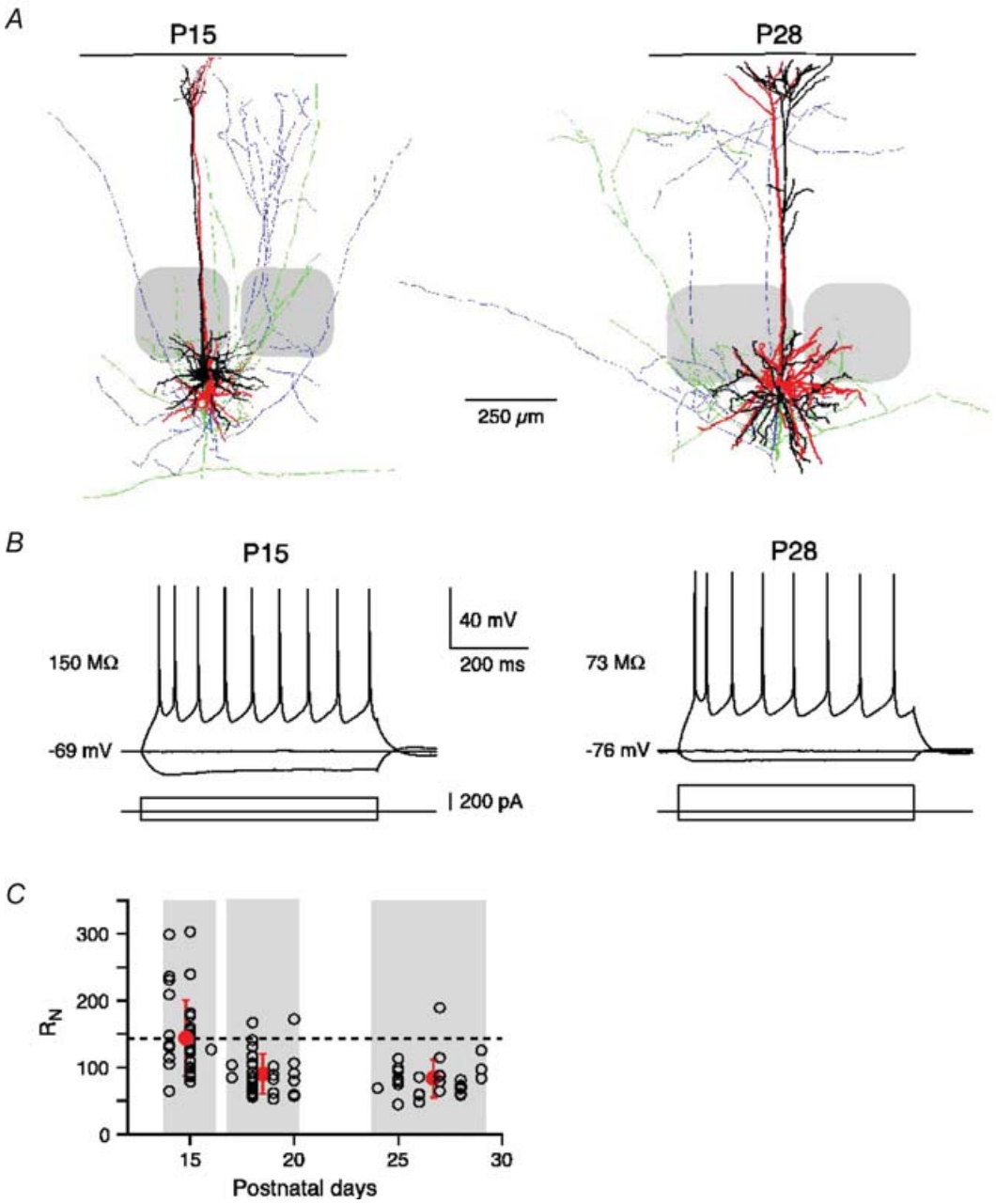

Figure 1. Developmental decrease in input resistance
A, neurolucida reconstruction of two synaptically connected pairs of layer 5A pyramidal neurons at P15 and P28. The dendritic and axonal arbors of the presynaptic (red and blue, respectively) and postsynaptic (white and green, respectively) neuron are shown. The soma–pia distances were 815 μm and 850 μm for the P15 pair, and 898 μm and 942 μm for the P28 pair. Barrels are indicated in grey. *B*, regular AP firing (upper traces) of L5A pyramidal neurons at P15 and P28 in response to current injections (lower traces). Note the more hyperpolarized resting membrane potential and lower input resistance (R_N) at P28. *C*, R_N decreases during postnatal development (2–4 weeks). Dashed line indicates the mean R_N value at P14–16 to emphasize the change in R_N with age.

traces 3 and 7 in Fig. 2*Aa*). The amplitude of 60 consecutive unitary EPSPs from the same examples is plotted in Fig. 2*Ab*, further emphasizing the developmental decrease in synaptic efficacy as well as an increase in variability and failure rate. The connection at P15 had a mean unitary EPSP amplitude of 1.50 ± 0.16 mV, a CV of 0.11 and a failure rate (FR) of 0% ($n = 60$ traces), whereas the connection at P28 had a mean unitary EPSP amplitude of 0.63 ± 0.32 mV, a CV of 0.5 and a FR of 10% ($n = 150$ traces).

The results from 80 similar experiments are summarized in Figs 2*B–D*, 3 and 4, and Table 1. Data from a total of 29 (P14–16), 27 (P17–20) and 24 (P24–29) pairs are included in the respective graphs. Histograms and mean

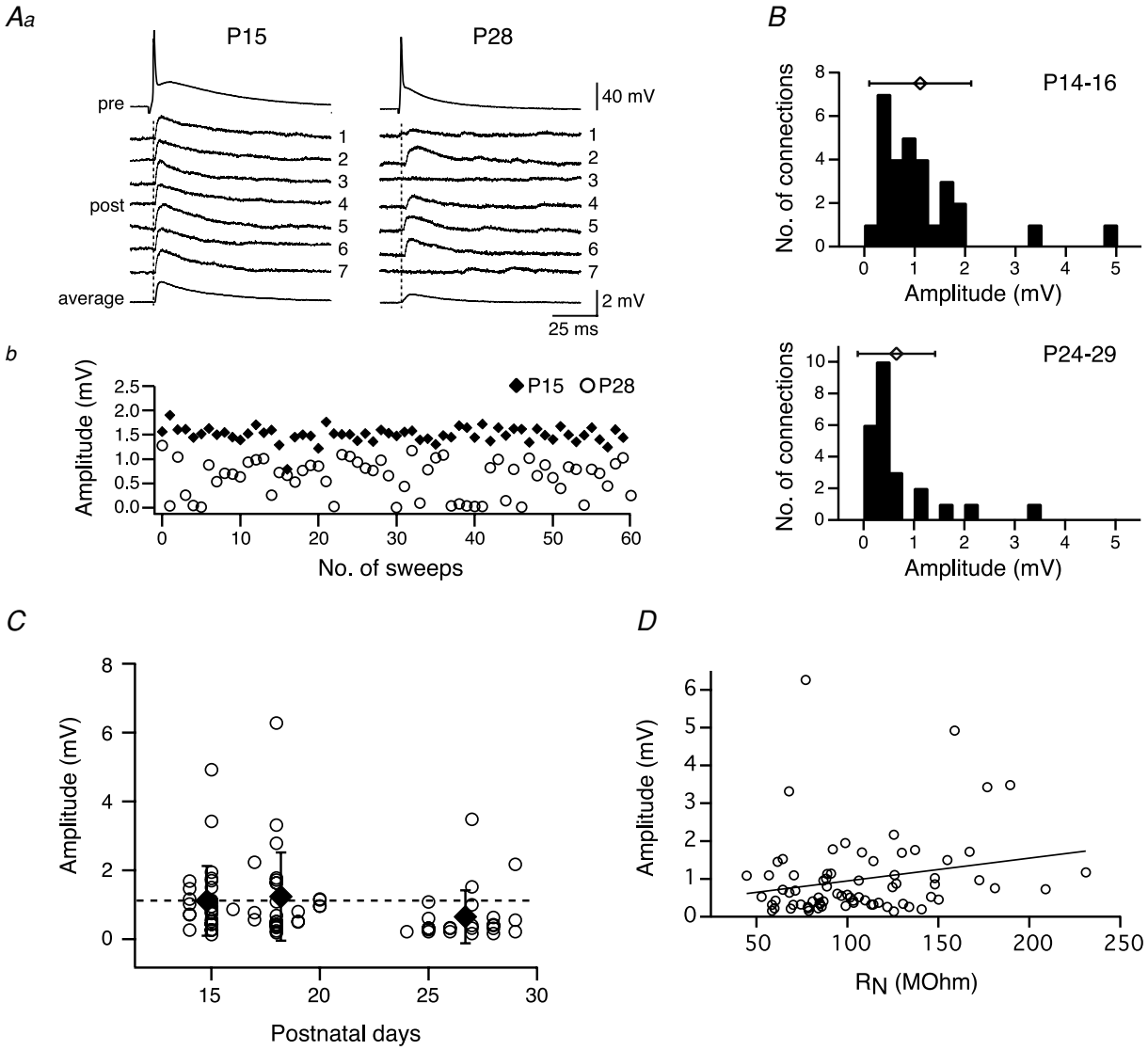

Figure 2. Efficacy of the L5A–L5A connection is age dependent
Aa, comparison of efficacy and variability evoked in L5A–L5A connections at P15 and P28. The presynaptic action potential (upper trace) and seven consecutive traces of the associated unitary EPSPs are shown for a connection at P15 and one at P28. The average EPSP waveform is shown at the bottom. *Ab*, EPSP amplitude plotted for 60 consecutive stimuli for the same pairs. Note the variability of the response and the occurrence of failures at P28. *B*, histograms for unitary EPSP amplitudes for two age groups, P14–16 and P24–29. Symbols above histograms give the mean (± S.D.) amplitude. Means were 1.1 ± 1.0 mV for P14–16 connections ($n = 29$) and 0.65 ± 0.77 mV for P24–29 connections ($n = 24$). *C*, unitary EPSP amplitude for each L5A–L5A connection and mean (± S.E.M.) amplitude for three age groups (P14–16, P17–20, P24–29) plotted as a function of postnatal days. Dotted line indicates the mean amplitude value at P14–16 to emphasize the decline in amplitude between 3 and 4 weeks of development. *D*, EPSP amplitudes are not correlated with the input resistance ($r = 0.2210$, $P = 0.0584$, Pearson correlation coefficient).

Table 1. Developmental changes in properties of synaptic connections and input resistance

Age	P14–16	P17–20	P24–29
Unitary EPSP (mV)	1.11 ± 1.01 ($n = 29$)	1.24 ± 1.28 ($n = 27$)	0.65 ± 0.77 ($n = 24$)*
Coefficient of variation	0.38 ± 0.20 ($n = 29$)	0.30 ± 0.16 ($n = 26$)	0.54 ± 0.20 ($n = 24$)**
Failure rate (%)	2.39 ± 4.08 ($n = 29$)	1.44 ± 3.29 ($n = 22$)	10.61 ± 8.68 ($n = 22$)**
PPR (%) ($EPSP_2/EPSP_1 \times 100$)	70.1 ± 16.6 ($n = 16$)	82.6 ± 10.8 ($n = 17$)*	103.8 ± 32.5 ($n = 21$)**
PPR (%) ($EPSP_3/EPSP_1 \times 100$)	60.2 ± 15.7 ($n = 16$)	66.9 ± 10.9 ($n = 17$)	98.3 ± 29.8 ($n = 21$)**
20–80% Rise time (ms)	1.84 ± 0.48 ($n = 19$)	1.35 ± 0.54 ($n = 23$)*	1.61 ± 0.36 ($n = 11$)
Decay time constant (ms)	25.9 ± 6.9 ($n = 19$)	17.8 ± 4.5 ($n = 18$)**	20.4 ± 7.4 ($n = 12$)*
Latency (ms)	1.24 ± 0.44 ($n = 16$)	1.07 ± 0.40 ($n = 20$)	1.15 ± 0.45 ($n = 9$)
Input resistance (MΩ)	144 ± 57 ($n = 37$)	90 ± 30 ($n = 33$)**	83 ± 28 ($n = 28$)**

Asterisks indicate statistically significant difference from the P14–16 age group (*$P < 0.05$, **$P < 0.005$).

values (±S.D.) of unitary EPSP amplitudes are plotted for P14–16 and P24–29 in Fig. 2*B*, demonstrating the broad range of amplitudes within a given population and their overall shift to the left as a function of age. At P14–16 (upper panel), unitary EPSP amplitude varied 35-fold for different connections of this population, ranging from 0.14 to 4.92 mV with a mean of 1.11 ± 1.01 mV. In comparison, at P24–29 unitary EPSP amplitude ranged from 0.16 to 3.48 mV (> 20-fold difference) and had a mean value of 0.65 ± 0.77 mV. These results together with our previous study (Frick *et al.* 2007) suggest that the efficacy of L5A–L5A connections is largest between 2 and 3 weeks postnatal with no significant difference within this developmental period (P14–16, 1.11 ± 1.01 mV, $n = 29$; P17–20, 1.24 ± 1.28 mV, $n = 27$; $P = 0.89$) (Fig. 2*C*). Between 3 and 4 weeks of cortical maturation, however, the amplitude of unitary EPSPs declined by approximately 40% as compared with both younger groups taken separately or combined (P24–29, 0.65 ± 0.77 mV, $n = 24$; P14–20, 1.17 ± 1.14 mV, $n = 56$, $P = 0.0011$). The unitary EPSP amplitudes for each experiment and the average values for the three age groups are plotted as a function of age in Fig. 2*C*, further emphasizing the decrease in amplitude between 3 and 4 weeks of age.

We next asked the question whether this strong decline in unitary EPSP amplitude could be a direct consequence of a decline in R_N during development (see above and Fig. 1*C*). While R_N generally influences the amplitude of EPSPs (Stuart & Spruston, 1998; Zhang, 2004), two findings argue against a major role of R_N in causing the observed developmental decrease in synaptic efficacy. First, the unitary EPSP amplitude was not correlated with R_N (Fig. 2*D*) ($r = 0.2210$, $P = 0.0584$, Pearson correlation coefficient), with a similar relationship for all ages (not shown). Second, the time course of the changes in R_N and EPSP amplitude showed no correlation; the major decline of R_N occurred between 2 and 3 weeks of age (~40%) with no change in EPSP amplitude, while the major decrease in amplitude (~40%) occurred during 3 and 4 weeks of age with only little drop in R_N (~8%).

Decrease in reliability of unitary EPSPs

As demonstrated in Fig. 2*A*, while the EPSP amplitude decreased, the variability (CV) and failure rate of unitary EPSPs increased during postnatal development. This is due to the inverse correlation between CV and EPSP amplitude as previously described for some neocortical connections (Markram *et al.* 1997; Feldmeyer *et al.* 1999, 2002, 2006; Frick *et al.* 2007). The changes in CV and failure rate are summarized in Fig. 3 and Table 1. Figure 3*A* shows the histograms and mean values for CV at P14–16 and at P24–29. At the younger age, CV was on average 0.38 ± 0.20 ($n = 29$), ranging from 0.11 to 0.96. The large CV at the upper end of the range resulted from a very low efficacy of this particular connection (unitary EPSP amplitude 0.14 mV). The CV was statistically larger at P24–29 averaging 0.54 ± 0.20 (range 0.14–0.78, $n = 24$; $P = 0.0029$). The developmental change in CV as a function of age is plotted in Fig. 3*C*, indicating that the CV is lowest for the age group P17–20 ($P = 0.1$ *versus* P14–16). This result suggests that, at least between 2 and 3 weeks postnatal, synaptic transmission at monosynaptic L5A–L5A connections is reliable (low CV) and characterized by a relatively high release probability (P_r).

This high reliability of synaptic transmission at the L5A–L5A connection in 2- to 3-week-old animals is also reflected in a low failure rate (Fig. 3*B* and *D*, Table 1). Histograms and mean values for the failure rate of synaptic transmission for P14–16 and P24–29 connections are plotted in Fig. 3*B*. At P14–16, 19 out of 29 connections displayed virtually no transmission failures (≤ 2%), and the mean failure rate was 2.4 ± 4.1% for all connections in this population, ranging from 0 to 18.6%. In more mature neocortex, however, approximately 10% of presynaptic APs failed to evoke a unitary EPSP, resulting in a decreased reliability of synaptic transmission (mean failure rate 10.6 ± 8.7%, range 0–16.3%, $n = 22$, $P = 0.0005$). In agreement with the results of the CV analysis, the failure rate was lowest at approximately 3 weeks of age and increased during the following week of development (Fig. 3*D*), further supporting maturation-dependent changes in

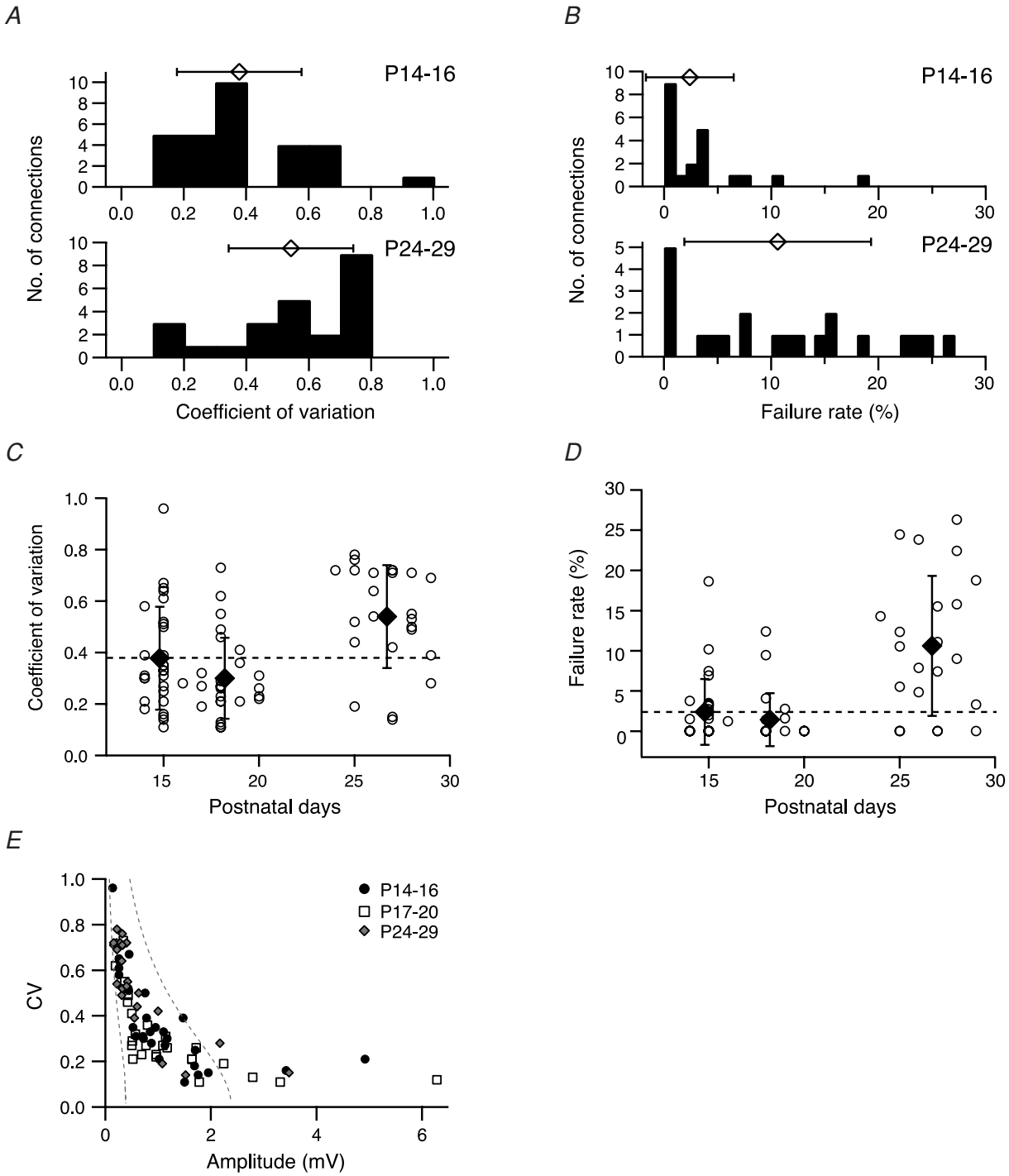

Figure 3. Development of variability and reliability
Histograms of coefficient of variation (CV, *A*) and failure rate (*B*) at two age groups (P14–16 and P24–29). Symbols above histograms give the mean (±S.D.) values. CV (*C*) and failure rate (*D*) for each L5A–L5A connection and mean (±S.D.) values for three age groups (P14–16, P17–20, P24–29) are plotted as function of postnatal days. Dotted line indicates the mean values at P14–16 to emphasize developmental changes in synaptic properties. Both CV and failure rate increase during the fourth week of maturation. *E*, CV plotted as function of EPSP amplitude assuming four synaptic contacts (close to the average number of contacts, Frick *et al*. 2007) and $q_S = 0.1$ mV (right curve) and $q_S = 0.6$ mV (left curve); P_r increases from 0.08 to 0.6 (right curve) and from 0.05 to 1.0 (left curve). The P_r values refer to the two endpoints of each curve. Connections with large mean EPSP amplitudes are not well described by binomial statistics. Note that the CV–EPSP function is similar for data from all three age groups.

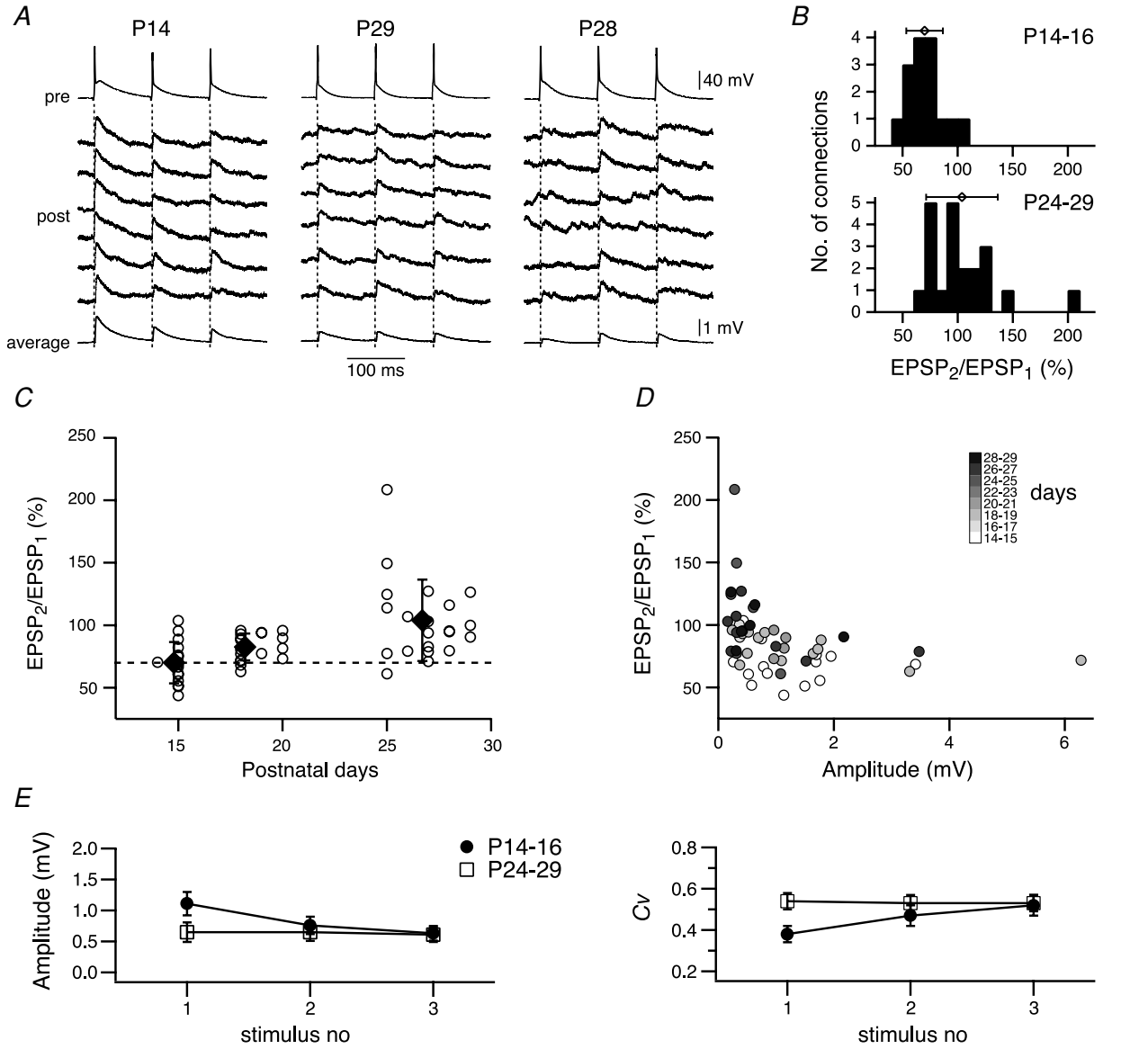

Figure 4. Change in short-term synaptic plasticity
A, comparison of short-term synaptic plasticity evoked in L5A–L5A connections at P14 (left column), P29 (middle column) and P28 (right column). Trains of three presynaptic action potentials at 10 Hz (upper trace) and six consecutive traces of associated EPSPs (lower traces) recorded in three L5A–L5A connections. The average EPSP waveform is shown at the bottom. The connection at P14 displayed strong depression, whereas the connections at P24–29 showed on average no change in short-term synaptic efficacy (middle column). In 50% of the P24–29 population paired-pulse facilitation was observed (right column). *B*, distribution of amplitude ratios (amplitude of second EPSP to amplitude of first EPSP, in per cent) for two age groups, P14–16 and P24–29. Symbols above histograms give the mean (±S.D.) amplitude ratios. Means were 70 ± 17% for P14–16 connections ($n = 16$) and 104 ± 33% for P24–29 connections ($n = 21$). *C*, amplitude ratios for each L5A–L5A connection and mean (±S.D.) values for three age groups (P14–16, P17–20, P24–29) are plotted as function of postnatal days. Dotted line indicates no short-term change. *D*, short-term synaptic plasticity depends on the intial EPSP amplitude and the age of the animal. Amplitude ratios are plotted as function of the initial EPSP amplitude and are greyscale-coded for the age in postnatal days. Note the shift in short-term change with age for similar initial EPSP amplitudes. *E*, release mechanisms in presynaptic terminals underlie short-term synaptic plasticity. Mean (± S.E.M.) amplitude (left graph) and mean (± S.E.M.) coefficient of variation (right graph) evoked during the first, second and third action potential in a train at P14–16 (●, $n = 16$ connections) and P24–29 (□, $n = 20$ connections). At P14–16 the EPSP amplitude decreased, whereas the CV increased, while for connections at P24–29 on average amplitude and CV showed no change. Note that amplitude and CV for both age groups reach similar values at the third stimulus.

the reliability of synaptic transmission at L5A–L5A connections. Figure 3*E* shows a plot of the CV values at all ages as a function of EPSP amplitude. Limiting curves (dashed line) assuming binomial release with

$$\mathrm{CV} = \sqrt{[(1 - P_r)/(n_b P_r)]} \text{ and } P_r = \Delta V/(n_b q_s)$$

were calculated assuming four release sites n_b (close to the mean number of putative synaptic contacts, 3.5 ± 1.8; Frick *et al.* 2007) and quantal amplitude q_S of 0.10 and 0.60 mV. Data from all ages fell inside the two limiting curves for EPSP amplitudes not exceeding 2 mV. This suggests that the observed shift in synaptic efficacy and reliability during maturation is more likely due a decrease in P_r and not the result of major changes in either q_S or the n_b.

Latency and time course of unitary EPSPs

We also analysed latency and kinetics of unitary EPSPs (Table 1). The latency varied up to 4-fold for different connections within each age group and was on average 1.24 ± 0.44 ms ($n = 16$), 1.07 ± 0.40 ms ($n = 20$) and 1.15 ± 0.45 ms ($n = 9$) for P14–16, P17–20 and P24–29, respectively. There was no significant correlation of unitary EPSP latency with the developmental stage of the cortical microcircuit ($P > 0.2$), and therefore data were pooled across all ages (1.15 ± 0.42, P14–29, $n = 45$). The decay time constant of unitary EPSPs, however, decreased by ~30% from 25.9 ± 6.9 ms at P14–16 ($n = 19$) to 17.8 ± 4.5 ms at P17–20 ($n = 18$) ($P = 0.0002$, unpaired *t* test), with no significant change during the following week (20.4 ± 7.4, $n = 12$; $P = 0.0125$ *versus* P14–16, $P = 0.31$ *versus* P17–20). The acceleration of the EPSP decay is probably due to a combination of the reduced membrane time constant (see above; for review, see e.g. Spruston *et al.* 1994), and a developmental change in the properties of the postsynaptic glutamate receptors (Carmignoto & Vicini, 1992; Burgard & Hablitz, 1993; Crair & Malenka, 1995; Flint *et al.* 1997; Stocca & Vicini, 1998).

Change in short-term plasticity of unitary EPSPs

We previously reported short-term synaptic depression at L5A–L5A connections in ~3-week-old animals (Frick *et al.* 2007). To test the hypothesis that both quality and quantity of short-term dynamics depend on the maturity of the cortical L5A microcircuit, we measured unitary EPSPs in response to triplets of presynaptic APs at interspike intervals (ISIs) of 100 ms as a function of age (Fig. 4). The reasons for using this ISI are 2-fold; first, the efficacy of synaptic transmission at many neocortical synapses changes on the hundreds of millisecond time scale (Zucker & Regehr, 2002). Second, temporal summation, which would otherwise confound our analysis (Banitt *et al.* 2005), is minimal at this rate. To quantify the degree of short-term changes of unitary EPSPs, we calculated the paired-pulse ratio of the EPSP amplitudes (PPR, see Methods), a value below 100% indicating short-term synaptic depression and a value above facilitation. The results from three experiments are illustrated in Fig. 4*A*. Six consecutive unitary EPSPs and the average response are shown for a connection at P14 (left panel), at P29 (middle panel) and at P28 (right panel). A typical finding from most of our experiments in young animals (P14–16) and represented in this example was that unitary EPSPs displayed depression in response to repetitive presynaptic APs. In this particular example, a PPR for the second EPSP of 51% and for the third EPSP of 48% was measured. The connection at P29 (middle panel), on the other hand, displayed no change in short-term dynamics (PPR for second EPSP 99%; PPR for third EPSP 93%) and is a representative example for the overall P24–29 population (see below). The connection at P28 (right panel) had small initial amplitude responses and some failures, and was characterized by synaptic facilitation, a feature shared by 43% of the P24–P29 population. In the example shown here, the PPR for the second EPSP was 208% and the PPR for the third EPSP 191%.

The results from 54 similar experiments are summarized in Fig. 4*B–D*, and Table 1. Data from a total of 16 (P14–16), 17 (P17–20) and 21 (P24–29) pairs are included in the respective graphs. Histograms and mean values for two age groups, P14–16 and P24–29, are plotted in Fig. 4*B*. For the P14–16 population, 15 out of 16 connections were characterized by short-term synaptic depression, the PPR ranging from 44% to 104%, with an average of 70 ± 17%. The third unitary EPSP amplitude decreased even stronger with a mean value of 60 ± 16% (range 36% to 89%). The more mature population was characterized by a large variability in short-term dynamics, ranging from strong depression (61%) to strong facilitation (208%) with a mean value of 104 ± 33% for the second EPSP. This PPR was significantly different when compared with P14–16 ($P = 0.0002$) or P17–20 (83 ± 11%, $P = 0.0153$). In this age population, there were no short-term changes for the third EPSP ($EPSP_3/EPSP_1$, 98 ± 30%, range 56% to 191%). In summary, the number of connections characterized by short-term facilitation increased from 6% at P14–16 to 43% at P24–29. This gradual change from short-term synaptic depression to facilitation during cortex maturation is also illustrated in Fig. 4*C*. One explanation for these results would be that the release probability (P_r) at L5A–L5A connections changes during development. To further support this idea, we analysed PPR as a function of both amplitude and age (Fig. 4*D*). It has been previously demonstrated for identified neocortical connections, that PPR is correlated with the amplitude of the first unitary EPSP (Tsodyks & Markram, 1997). Simplistically, synapses with a low P_r

display facilitation, whereas synapses with a high P_r exhibit depression (Thomson, 2003). Figure 4*D* demonstrates that PPR depends not only on the EPSP amplitude, but also on age, leading to larger PPR values for equal amplitudes at more mature compared with young ages. This finding provides further evidence for a decrease in P_r during maturation.

What are the consequences of the observed changes in the quality of short-term synaptic plasticity for the spread of activity in the local L5A circuits? In Fig. 4*E* we plotted the mean values for the amplitude and CV of EPSPs evoked during the first, second and third AP in a train for P14–16 and P24–29 connections. For the first EPSP, amplitude and CV are as described earlier and illustrated in Figs 2 and 3, namely a larger amplitude and a smaller CV at P14–16 as compared with P24–29. Somewhat surprisingly, though, is the fact that amplitude and CV for the third EPSP in the train are the same for both age groups, suggesting that under some conditions of repetitive firing activity the efficacy of synaptic transmission during such a train may be similar for both young and more mature L5A connections.

Discussion

Our study demonstrates that maturation leads to pathway-specific functional changes at local excitatory connections in the barrel columns of rats. We found that for the networks of layer 5A pyramidal neurons the input resistance along with the decay time constant of unitary EPSPs declined during the 3rd week of postnatal development. More importantly, the efficacy of these connections was significantly reduced during the 4th week of maturation, and was accompanied by a decrease in the reliability of synaptic transmission and a change in short-term dynamics from depression to slight facilitation. The precise cellular/synaptic mechanisms underlying the developmental changes in the synaptic properties between L5A pyramidal neurons during maturation remain to be elucidated, but our analysis indicates that a change in the presynaptic transmitter release probability could explain some of the observed modifications.

Synapse formation and elimination during development

Cortical networks such as columns and maps are established during development by the specific formation, elimination and rearrangement of synaptic connections between neurons located in the same and different cortical layers (Goodman & Shatz, 1993; Katz & Shatz, 1996). The formation of synaptic contacts (synaptogenesis) in the neocortex is maximal during the second and third postnatal week (P11–20) and coincides with the formation of most spines on the dendrites (Parnavelas & Globus, 1976; Parnavelas *et al.* 1978; De Felipe *et al.* 1997; Marrone & Petit, 2002). Following this period, some of the synapses are selectively eliminated, resulting in a balanced state that assures optimal network functioning (Chechik *et al.* 1999). This net elimination of synapses affects mainly asymmetrical (putatively excitatory) synapses and therefore excitatory circuits (Rakic *et al.* 1994; Seeger *et al.* 2005) and has been observed in rhesus monkeys (Rakic *et al.* 1986). Elimination is, however, more controversial for rodents (Aghajanian & Bloom, 1967; Blue & Parnavelas, 1983; Micheva & Beaulieu, 1996; De Felipe *et al.* 1997). Two studies of somatosensory cortex in mice and in rats (here: barrel field) showed a slight decrease in the synapse number after reaching a maximum at P20–30 (Micheva & Beaulieu, 1996; De Felipe *et al.* 1997), but others reported no significant overproduction of synapses in rat somatosensory cortex between P5 and P60 (Blue & Parnavelas, 1983). It is, however, important to bear in mind that the time course and pattern of cortical synaptogenesis might depend on the specific pathways and cannot be generalized across layers and cell types. Our results suggest a fairly high synaptic efficacy for L5A pyramidal neuron connections between 2 and 3 weeks of postnatal age and a significant reduction during the following week of postnatal development. Whether or not a change in synapse number at individual L5A–L5A connections occurs during development and contributes to the measured changes in efficacy remains speculative and can only be determined at the resolution of electron microscopy using large sample numbers. From the aforementioned studies and our own data we conclude that functional synaptic changes are more likely to be the major cause for altering the synaptic properties at L5A pyramidal neuron connections (see below).

Weakening of local L5A connections during maturation

Our data show that functional changes occur at unitary connections between layer 5A pyramidal neurons during postnatal development, resulting in a decrease in the efficacy and reliability of synaptic transmission, as well as a change in the short term dynamics. The most parsimonious explanation for our results is that development leads to functional changes at existing synaptic contacts. One cannot, however, exclude the possibility that synapse turnover (Trachtenberg *et al.* 2002; Zuo *et al.* 2005; De Paola *et al.* 2006) results in new, weaker synapses being formed during development. We found a significant drop in the mean amplitude of unitary EPSPs from ∼1.2 mV at P14–20 to ∼0.7 mV at P24–29, a tendency also mentioned in a study on connections between L5B pyramidal neurons (Reyes & Sakmann, 1999). The decrease in synaptic efficacy was accompanied by a larger variability/failure rate of synaptic transmission, i.e. an altered reliability of transmission. However, as

Fig. 3*E* demonstrates, the decrease in synaptic efficacy and reliability during maturation is less likely the result of major changes in either quantal amplitude (q_S) or the number of synaptic contacts (n_b) but rather due to a decrease in the release probability (P_r). Such a decline in P_r during maturation has also been suggested to occur at hippocampal CA3–CA1 (Bolshakov & Siegelbaum, 1995), cortico-striatal (Choi & Lovinger, 1997), cerebellar (Pouzat & Hestrin, 1997), and other neocortical (Angulo *et al.* 1999; Reyes & Sakmann, 1999) connections.

Developmental change in short-term dynamics

The efficacy of synaptic transmission at many neocortical synapses changes when presynaptic APs are triggered at interspike intervals on time scales ranging approximately from a millisecond to a second, leading to either a decrease (depression) or increase (facilitation) in the EPSP amplitude (e.g. Thomson *et al.* 1993; Markram *et al.* 1998; Angulo *et al.* 1999; Reyes & Sakmann, 1999; Feldmeyer *et al.* 2002; for review see Zucker & Regehr, 2002). These short-term changes of synaptic efficacy depend on the target cell identities (Markram *et al.* 1998; Reyes *et al.* 1998; Kozloski *et al.* 2001; Koester & Johnston, 2005) and are caused by mechanisms that regulate the Ca^{2+} dependence of transmitter release or synaptic response (Zucker & Regehr, 2002). Simplistically, synapses with a low P_r display facilitation, whereas synapses with a high P_r exhibit depression (Thomson, 2003) although release probability-independent paired-pulse behaviour has been reported (Rozov *et al.* 2001; Thomson, 2003). In our study, ∼95% of the young connections (P14–16) displayed synaptic depression, and the degree of depression was largely determined by the initial P_r as shown by the relation of PPR and amplitude. During the following 2 weeks of postnatal development we found a progressive change in the short-term synaptic plasticity towards facilitation, reflecting a progressive modification in the initial P_r. This change in short-term synaptic plasticity at L5A–L5A connections is in accordance with previous findings for connections between L5B pyramidal neurons (Reyes & Sakmann, 1999), emphasizing its importance for the spread of activity within the cortical circuits during development. What is remarkable, though, is the high variability of PPR in the more mature cortex (P24–29), ranging from strong depression (PPR = 0.6) to strong facilitation (PPR = 2.1), indicating a large diversity in P_r at this age. This synaptic property might reflect their recent history of activity, conferring the synapses with a variety of filter properties and a diversity of computations (Abbott & Regehr, 2004; Destexhe & Marder, 2004; Richardson *et al.* 2005). Although the PPR inversely correlates with the first unitary EPSP amplitude (see above), the differences in amplitudes for young and more mature connections cannot account for the differences in short-term dynamics, because they are significantly different even for EPSPs of equal size (see Fig. 4*D*), again arguing for a change in initial P_r.

In vivo recordings from neocortical neurons, including L5A pyramidal neurons, have demonstrated that interspike intervals at time scales relevant to induce short-term synaptic plasticity exist during both spontaneous and evoked activity (Armstrong-James *et al.* 1994; Huang *et al.* 1998; Brecht & Sakmann, 2002; Manns *et al.* 2004; Wilent & Contreras, 2004; de Kock *et al.* 2007). This highlights the physiological significance of developmental changes in short-term plasticity for the spread of excitation originating from L5A pyramidal neurons. In young neocortex (2 to 3 weeks) single APs would be efficiently transmitted in this network, while firing activity at frequencies as low as 10 Hz would lead to successive depression of unitary EPSPs within these trains. On the other hand, in more mature animals, synaptic transmission at ∼45% of the L5A–L5A connections would be more efficiently transmitted with trains of APs at higher frequencies due to facilitating synaptic properties. Furthermore, our data suggest that during certain AP firing patterns the strength and variability of synaptic transmission within this AP train reach similar values for young and more mature animals (see Fig. 4*E*).

Conclusions

In summary, our results strongly suggest that synaptic transmission at unitary connections between L5A pyramidal neurons is characterized by a decline of release probability during maturation. This functional change is most prominent after the third postnatal week, and raises the question whether such developmental alterations are a general feature for neocortical and extra-cortical connections. This would have important implications for models of cortical microcircuit signalling, the properties of which have so far been mainly characterized at younger ages. It may be that a higher reliability and efficacy of synaptic transmission as well as the longer EPSP duration in immature cortical circuits is required for the formation and maintenance of specific synaptic connections. Thus, unitary connections in immature tissue are tuned to provide larger and longer signals that may stabilize immature synapses thereby converting them into mature ones in an activity-dependent manner.

On the other hand, the fact that L5A connections in more mature cortex have a large variability in their release probability and in their concomitant short-term dynamics may suggest that they have been specifically tuned by preceding activity. This would increase the possible range of computational functions and therefore diversity of signalling in cortical circuits, and appears to be an important step in the functional maturation of excitatory synapses in the neocortex.

References

Abbott LF & Regehr WG (2004). Synaptic computation. *Nature* **431**, 796–803.

Aghajanian GK & Bloom FE (1967). The formation of synaptic junctions in developing rat brain: a quantitative electron microscopic study. *Brain Res* **6**, 716–727.

Ahissar E, Sosnik R, Bagdasarian K & Haidarliu S (2001). Temporal frequency of whisker movement. II. Laminar organization of cortical representations. *J Neurophysiol* **86**, 354–367.

Alloway KD, Crist J, Mutic JJ & Roy SA (1999). Corticostriatal projections from rat barrel cortex have an anisotropic organization that correlates with vibrissal whisking behavior. *J Neurosci* **19**, 10908–10922.

Alloway KD, Zhang M & Chakrabarti S (2004). Septal columns in rodent barrel cortex: functional circuits for modulating whisking behavior. *J Comp Neurol* **480**, 299–309.

Angulo MC, Staiger JF, Rossier J & Audinat E (1999). Developmental synaptic changes increase the range of integrative capabilities of an identified excitatory neocortical connection. *J Neurosci* **19**, 1566–1576.

Armstrong-James M, Diamond ME & Ebner FF (1994). An innocuous bias in whisker use in adult rats modifies receptive fields of barrel cortex neurons. *J Neurosci* **14**, 6978–6991.

Banitt Y, Martin KAC & Segev I (2005). Depressed responses of facilitatory synapses. *J Neurophysiol* **94**, 865–870.

Blue ME & Parnavelas JG (1983). The formation and maturation of synapses in the visual cortex of the rat. I. Qualitative analysis. *J Neurocytol* **121**, 599–616.

Bolshakov VY & Siegelbaum SA (1995). Regulation of hippocampal transmitter release during development and long-term potentiation. *Science* **269**, 1730–1734.

Brecht M & Sakmann B (2002). Dynamic representation of whisker deflection by synaptic potentials in spiny stellate and pyramidal cells in the barrels and septa of layer 4 rat somatosensory cortex. *J Physiol* **543**, 49–70.

Bureau I, von Saint Paul F & Svoboda K (2006). Interdigitated paralemniscal and lemniscal pathways in the mouse barrel cortex. *PLOS Biol* **4**, 2361–2371.

Burgard EC & Hablitz JJ (1993). Developmental changes in NMDA and non-NMDA receptor-mediated synaptic potentials in rat neocortex. *J Neurophysiol* **69**, 230–240.

Carmignoto G & Vicini S (1992). Activity-dependent decrease in NMDA receptor responses during development of the visual cortex. *Science* **258**, 1007–1011.

Chechik G, Meilijson I & Ruppin E (1999). Neuronal regulation: a mechanism for synaptic pruning during brain maturation. *Neural Comput* **11**, 2061–2080.

Chmielowska J, Carvell GE & Simons DJ (1989). Spatial organization of thalamocortical and corticothalamic projection systems in the rat SmI barrel cortex. *J Comp Neurol* **285**, 325–338.

Choi S & Lovinger DM (1997). Decreased probability of neurotransmitter releas underlies striatal long-term depression and postnatal development of corticostriatal synapses. *Proc Natl Acad Sci U S A* **94**, 2665–2670.

Cohen-Cory S (2002). The developing synapse: construction and modulation of synaptic structures and circuits. *Science* **298**, 770–776.

Crair MC & Malenka RC (1995). A critical period for long-term potentiation at thalamocortical synapses. *Nature* **375**, 325–328.

De Felipe J, Marco P, Fairen A & Jones EG (1997). Inhibitory synaptogenesis in mouse somatosensory cortex. *Cereb Cortex* **7**, 619–634.

de Kock CPJ, Bruno RM, Spors H & Sakmann B (2007). Layer- and cell-type-specific suprathreshold stimulus representation in rat primary somatosensory cortex. *J Physiol* **581**, 139–154.

De Paola V, Holtmaat A, Knott G, Song S, Wilbrecht L, Caroni P & Svoboda K (2006). Cell type-specific structural plasticity of axonal branches and boutons in the adult neocortex. *Neuron* **49**, 861–875.

Destexhe A & Marder E (2004). Plasticity in single neuron and circuit computation. *Nature* **431**, 789–795.

Donoghue JP & Parham C (1983). Afferent connections of the lateral agranular field of the rat motor cortex. *J Comp Neurol* **217**, 390–404.

Douglas RJ & Martin KA (2004). Neuronal circuits of the neocortex. *Annu Rev Neurosci* **27**, 419–451.

Feldmeyer D, Egger V, Lübke J & Sakmann B (1999). Reliable synaptic connections between pairs of excitatory layer 4 neurones within a single 'barrel' of developing rat somatosensory cortex. *J Physiol* **575**, 583–602.

Feldmeyer D, Lübke J & Sakmann B (2006). Efficacy and connectivity of intracolumnar pairs of layer 2/3 pyramidal cells in the barrel cortex of juvenile rats. *J Physiol* **575**, 582–602.

Feldmeyer D, Lübke J, Silver RA & Sakmann B (2002). Synaptic connections between layer 4 spiny neurone–layer 2/3 pyramidal cell pairs in juvenile rat barrel cortex: physiology and anatomy of interlaminar signalling within a cortical column. *J Physiol* **538**, 803–822.

Feldmeyer D, Roth A & Sakmann B (2005). Monosynaptic connections between pairs of spiny stellate cells in layer 4 and pyramidal cells in layer 5A indicate that lemniscal and paralemniscal afferent pathways converge in the infragranular somatosensory cortex. *J Neurosci* **25**, 3423–3431.

Flint AC, Maisch US, Weishaupt JH, Kriegstein AR & Monyer H (1997). NR2A subunit expression shortens NMDA receptor synaptic currents in developing neocortex. *J Neurosci* **17**, 2469–2476.

Frick A, Feldmeyer D, Helmstaedter M & Sakmann B (2007). Monosynaptic connections between pairs of L5A pyramidal neurons in columns of juvenile rat somatosensory cortex. *Cerebral Cortex*; DOI: 10.1093/cercor/bhm074.

Garner CC, Waites CL & Ziv NE (2006). Synapse development: still looking for the forest, still lost in the trees. *Cell Tissue Res* **326**, 249–262.

Goodman CS & Shatz CJ (1993). Developmental mechanisms that generate precise patterns of neuronal connectivity. *Cell* **72** (Suppl.), 77–98.

Hoffer ZS, Arantes HB, Roth RL & Alloway KD (2005). Functional circuits mediating sensorimotor integration: quantitative comparisons of projections from rodent barrel cortex to primary motor cortex, neostriatum, superior colliculus, and the pons. *J Comp Neurol* **488**, 82–100.

Huang W, Armstrong-James M, Rema V, Diamond ME & Ebner FF (1998). Contribution of supragranular layers to sensory processing and plasticity in adult rat barrel cortex. *J Neurophysiol* **80**, 3261–3271.

Katz LC & Shatz CJ (1996). Synaptic activity and the construction of cortical circuits. *Science* **274**, 1133–1138.

Koester HJ & Johnston D (2005). Target cell-dependent normalization of transmitter release at neocortical synapses. *Science* **308**, 863–866.

Koralek KA, Olavarria J & Killackey HP (1990). Areal and laminar organization of corticocortical projections in the rat somatosensory cortex. *J Comp Neurol* **299**, 133–150.

Kozloski J, Hamzei-Sichani F & Yuste R (2001). Stereotyped position of local synaptic targets in neocortex. *Science* **293**, 868–872.

Larsen DD & Callaway EM (2006). Development of layer-specific axonal arborizations in mouse primary somatosensory cortex. *J Comp Neurol* **494**, 398–414.

Lübke J & Feldmeyer D (2007). Excitatory signal flow and connectivity in a cortical column: focus on barrel cortex. *Brain Struct Funct* **212**, 3–17.

Lübke J, Roth A, Feldmeyer D & Sakmann B (2003). Morphometric analysis of the columnar innervation domain of neurons connecting layer 4 and layer 2/3 of juvenile rat barrel cortex. *Cereb Cortex* **13**, 1051–1063.

Manns ID, Sakmann B & Brecht M (2004). Sub- and suprathreshold receptive field properties of pyramidal neurones in layers 5A and 5B of rat somatosensory barrel cortex. *J Physiol* **556**, 601–622.

Markram H, Lübke J, Frotscher M, Roth A & Sakmann B (1997). Physiology and anatomy of synaptic connections between thick tufted pyramidal neurones in the developing rat neocortex. *J Physiol* **500**, 409–440.

Markram H, Wang Y & Tsodyks M (1998). Differential signaling via the same axon of neocortical pyramidal neurons. *Proc Natl Acad Sci U S A* **95**, 5323–5328.

Marrone DF & Petit DL (2002). The role of synaptic morphology in neural plasticity: structural interactions underlying synaptic power. *Brain Res Rev* **38**, 291–308.

Mercier BE, Legg CR & Glickstein M (1990). Basal ganglia and cerebellum receive different somatosensory information in rats. *Proc Natl Acad Sci U S A* **87**, 4388–4392.

Micheva KD & Beaulieu C (1996). Quantitative aspects of synaptogenesis in the rat barrel field cortex with special reference to GABA circuitry. *J Comp Neurol* **373**, 340–354.

Mountcastle VB (1997). The columnar organization of the neocortex. *Brain* **120**, 701–722.

Nelson SB (2002). Cortical microcircuits: diverse or canonical? *Neuron* **36**, 19–27.

Parnavelas JG, Bradford R, Mounty EJ & Lieberman AR (1978). The development of non-pyramidal neurons in the visual cortex of the rat. *Anat Embryol (Berl)* **155**, 1–14.

Parnavelas JG & Globus A (1976). The effect of continuous illumination on the development of cortical neurons in the rat: a Golgi study. *Exp Neurol* **51**, 637–647.

Pouzat C & Hestrin S (1997). Developmental regulation of basket/stellate cell–Purkinje cell synapses in the cerebellum. *J Neurosci* **17**, 9104–9112.

Rakic P, Bourgeois JP, Eckenhoff MF, Zecevic N & Goldman-Rakic PS (1986). Concurrent overproduction of synapses in diverse regions of the primate cerebral cortex. *Science* **231**, 232–235.

Rakic P, Bourgeois J-P & Goldman-Rakic PS (1994). Synaptic development of the cerebral cortex: implications for learning, memory and mental illness. *Progr Brain Res* **102**, 227–243.

Reyes A, Lujan R, Rozov A, Burnashev N, Somogyi P & Sakmann B (1998). Target-cell-specific facilitation and depression in neocortical circuits. *Nat Neurosci* **1**, 279–285.

Reyes A & Sakmann B (1999). Developmental switch in the short-term modification of unitary EPSPs evoked in layer 2/3 and layer 5 pyramidal neurons of rat neocortex. *J Neurosci* **19**, 3827–3835.

Richardson MJE, Melamed O, Silberberg G, Gerstner W & Markram H (2005). Short-term synaptic plasticity orchestrates the response of pyramidal cells and interneurons to population bursts. *J Comput Neurosci* **18**, 323–331.

Rozov A, Jerecic J, Sakmann B & Burnashev N (2001). AMPA receptor channels with long-lasting desensitization in bipolar interneurons contribute to synaptic depression in a novel feedback circuit in layer 2/3 or rat neocortex. *J Neurosci* **21**, 8062–8071.

Schubert D, Kötter R, Luhmann HJ & Staiger JF (2006). Morphology, electrophysiology and functional input connectivity of pyramidal neurons characterizes a genuine layer Va in the primary somatosensory cortex. *Cereb Cortex* **16**, 223–236.

Seeger G, Gärtner U & Arendt T (2005). Transgenic activation of Ras in neurons increases synapse formation in mouse neocortex. *J Neural Transm* **112**, 751–761.

Silberberg G, Grillner S, LeBeau FEN, Maex R & Markram H (2005). Synaptic pathways in neural microcircuits. *Trends Neurosci* **28**, 541–551.

Spruston N, Jaffe DB & Johnston D (1994). Dendritic attenuation of synaptic potentials and currents: the role of passive membrane properties. *Trends Neurosci* **17**, 161–166.

Stocca G & Vicini S (1998). Increased contribution of NR2A subunit to synaptic NMDA receptors in developing rat cortical neurons. *J Physiol* **507**, 13–24.

Stuart G & Spruston N (1998). Determinants of voltage attenuation in neocortical pyramidal neuron dendrites. *J Neurosci* **18**, 3501–3510.

Thomson AM (2003). Presynaptic frequency- and pattern-dependent filtering. *J Comput Neurosci* **15**, 159–202.

Thomson AM, Deuchars J & West DC (1993). Single axon excitatory postsynaptic potentials in neocortical interneurons exhibit pronounced paired pulse facilitation. *Neurosci* **54**, 347–360.

Trachtenberg JT, Chen BE, Knott GW, Feng G, Sanes JR, Welker E & Svoboda K (2002). Long-term in vivo imaging of experience-dependent synaptic plasticity in adult cortex. *Nature* **420**, 788–794.

Tsodyks MV & Markram H (1997). The neural code between neocortical pyramidal neurons depends on neurotransmitter release probability. *Proc Natl Acad Sci U S A* **94**, 719–723.

Watts J & Thomson AM (2005). Excitatory and inhibitory connections show selectivity in the neocortex. *J Physiol* **562**, 89–97.

Wilent WB & Contreras D (2004). Synaptic responses to whisker deflections in rat barrel cortex as a function of cortical layer and stimulus intensity. *J Neurosci* **24**, 3985–3998.

Wise SP & Jones EG (1977). Cells of origin and terminal distribution of descending projections of the rat somatic sensory cortex. *J Comp Neurol* **175**, 129–157.

Wong-Riley M (1979). Changes in the visual system of monocularly sutured or enucleated cats demonstrable with cytochrome oxidase histochemistry. *Brain Res* **171**, 11–28.

Woolsey TA & van der Loos H (1970). The structural organization of layer IV in the somatosensory region (SI) of mouse cerebral cortex. The description of a cortical field composed of discrete cytoarchitectonic units. *Brain Res* **17**, 205–242.

Zhang ZW (2004). Maturation of layer V pyramidal neurons in the rat prefrontal cortex: intrinsic properties and synaptic function. *J Neurophysiol* **91**, 1171–1182.

Zilles K & Wree A (1995). Cortex: areal and laminar structure. In *The Rat Nervous System*, ed. Paxinos G, pp. 649–685. Academic Press, New York.

Zucker RS & Regehr WG (2002). Short-term synaptic plasticity. *Annu Rev Physiol* **64**, 355–405.

Zuo Y, Lin A, Chang P & Gan WB (2005). Development of long-term dendritic spine stability in diverse regions of cerebral cortex. *Neuron* **46**, 181–189.

Acknowledgements

We would like to thank Drs Gabriele Radnikow and Randy Bruno for comments on the manuscript. Support was provided by the Max Planck Society.